$Sn_2Br_xI_{4-x}$(g) and $Sn_2Br_yI_{3-y}^+$ ($x = 0-4$, $y = 0-3$) Species: Mass Spectrometric Evidence and Quantum-Chemical Studies

J. Saloni,[†,‡] S. Roszak,*[,†,‡] M. Miller,[§] K. Hilpert,[||] and J. Leszczynski[‡]

Institute of Physical and Theoretical Chemistry, Wroclaw University of Technology, Wybrzeże Wyspiańskiego 27, 50-370 Wroclaw, Poland, Institute of Inorganic Chemistry and Metallurgy of Rare Elements, Wroclaw University of Technology, Wybrzeże Wyspiańskiego 27, 50-370 Wroclaw, Poland, Research Centre Jülich, Institute for Materials and Processes in Energy Systems, 52425 Jülich, Germany, and Computational Centre for Molecular Structure and Interactions, Jackson State University, Jackson, Mississippi 39217

Received: September 25, 2003; In Final Form: January 31, 2004

Dimeric gaseous species $Sn_2Br_xI_{4-x}$, $x = 0-4$, were detected by Knudsen effusion mass spectrometry. Fragment ionic species $Sn_2Br_yI_{3-y}^+$, $y = 0-3$, yielded by electron bombardment were identified in mass spectra of $SnBr_2-SnI_2$ equilibrium vapors. The structure and bonding of identified ions and neutral precursors were studied by quantum-chemical methods. Enthalpies and entropies of the anion-exchange reactions involving gaseous dimeric species were estimated by the use of mass spectrometric and theoretical data. Implications of the thermodynamic and structural data obtained by theoretical methods on the observed fragmentation paths of the neutral $Sn_2Br_xI_{4-x}$ species are discussed. The nature of interactions leading to dimer formation is studied on the basis of the atomic charge distribution and the variational-perturbational interaction energy decomposition scheme. The studies unravelled the additivity of properties such as bond length, vibrational frequencies, and atomic charge distribution corresponding to Sn−Br and Sn−I bonds participating in studied molecules and ions.

1. Introduction

Metal halides are known to form various kinds of halogen-bridged vapor complexes.[1−3] These complexes are important for practical applications[1] and provide challenging targets for basic research.[3] Despite many experimental studies carried out mostly by the Knudsen effusion mass spectrometry, still little is known about the nature of chemical bonding and the structure of the metal halide complex. Knowledge concerning fragmentation processes of such species upon electron bombardment—the ionization technique commonly used in the Knudsen effusion mass spectrometry is rather scanty as well. Measurements lead to uncertainties in data obtained by this method due to difficulties in the assignment of ion intensities to their neutral precursors.[4,5] This is particularly the case for the minor vapor components for which fragmentation studies based on recording ionization efficiency curves, or on the isothermal evaporation method, are difficult to apply.

In our previous study we investigated the thermochemistry of monomer species present in $SnBr_2-SnI_2$ vapors.[6] In this work we report the mass spectrometric identification of dimeric species in the $SnBr_2-SnI_2$ system. Quantum-chemical studies were performed for neutral $Sn_2Br_xI_{4-x}$ complexes that correspond to $Sn_2Br_yI_{3-y}^+$ fragment ions detected in the mass spectrum. Data obtained from both experimental and theoretical sources resulted in the prediction of the structural parameters of molecular and ionic species and in thermodynamic data of gaseous equilibria involving the $Sn_2Br_xI_{4-x}$ dimer complexes. Studies of the nature of bonding by terminal and bridged bonds were performed to elucidate the differences between Sn−Br and Sn−I bonds in different environments.

2. Experimental Section

Mass spectrometric studies were carried out with a substantially modified single-focusing CH5 mass spectrometer (Finnigan MAT, Bremen, Germany)[7] which was equipped with the Knudsen cell machined from molybdenum of a knife-edged effusion orifice with a diameter of 0.8 mm. Temperatures were measured with a chromel/alumel thermocouple calibrated at the melting point of silver. Electrons with energy of 25 eV were used for the ionization of neutral vapors.

$SnBr_2$ and SnI_2 (both nominal purity 99.999% mass, Cerac Inc., Milwaukee, WI) were used for the sample preparation. Three samples of different chemical compositions were prepared (Table 1). The compositions were chosen on the basis of the $SnBr_2-SnI_2$ phase diagram,[8] ensuring the different vapor composition and, as a consequence, different mass spectra of equilibrium vapors. Stoichiometric amounts of components were mixed and put into the Knudsen cell without the previous melting. After heating, samples were kept at a temperature of 400 K with the simultaneous recording of the mass spectrum. After the ion intensity became time-independent, mass spectra were recorded at different temperatures. Runs 2 and 5 were carried out by the use of the same material as the one used in runs 1 and 4, respectively. The partial depletion of the more volatile SnI_2 from initial samples during the vaporization study resulted in somewhat different mass spectra obtained in two experiments with the same nominal chemical composition.

* Corresponding author. E-mail: roszak@mml.ch.pwr.wroc.pl.
[†] Institute of Physical and Theoretical Chemistry, Wroclaw University of Technology.
[‡] Jackson State University.
[§] Institute of Inorganic Chemistry and Metallurgy of Rare Elements, Wroclaw University of Technology.
[||] Institute for Materials and Processes in Energy Systems.

10.1021/jp036866j CCC: $27.50
Published on Web 03/09/2004

TABLE 1: Ion Intensities of Dimeric Species (in Arbitrary Units) Recorded upon Vaporizing the $SnBr_2-SnI_2$ Samples of Different Compositions

	Sn_2Br_4(g)	Sn_2Br_3I	$Sn_2Br_2I_2$	Sn_2BrI_3	Sn_2I_4
T/K	$I(Sn_2Br_3^+)$	$I(Sn_2Br_2I^+)$	$I(Sn_2BrI_2^+)$	$I(Sn_2I_3^+)$	
Run 1		$x(SnBr_2) = 0.462$			
573	1.55E+04	1.48E+04	5.82E+03	1.43E+03	
563	1.28E+04	1.12E+04	4.37E+03	1.17E+03	
553	8.39E+03	7.02E+03	3.39E+03	6.66E+02	
543	6.39E+03	5.47E+03	2.73E+03	4.97E+02	
533	3.86E+03	3.20E+03	1.63E+03	2.98E+02	
523	2.71E+03	2.05E+03	9.77E+02	1.76E+02	
513	1.69E+03	1.09E+03	3.56E+02	5.77E+01	
503	6.80E+02	3.92E+02	1.60E+02	2.14E+01	
493	2.61E+02	1.59E+02	5.42E+01	9.69E+00	
483	8.95E+01	5.69E+01	2.14E+01	4.72E+00	
473	3.56E+01	1.74E+01	8.59E+00		
Run 2		$x(SnBr_2) = 0.462$			
583	2.11E+04	2.12E+04	1.46E+04	3.09E+03	
573	1.59E+04	1.55E+04	1.00E+04	2.06E+03	
563	1.04E+04	9.54E+03	6.38E+03	1.32E+03	
553	8.35E+03	7.20E+03	4.52E+03	9.29E+02	
543	5.50E+03	4.46E+03	2.83E+03	6.31E+02	
533	3.17E+03	2.71E+03	1.68E+03	2.99E+02	
523	2.01E+03	1.65E+03	8.64E+02	1.35E+02	
513	1.06E+03	7.14E+02	4.12E+02	5.91E+01	
503	4.18E+02	3.00E+02	1.49E+02	1.86E+01	
493	1.60E+02	1.06E+02	5.09E+01	5.72E+00	
483	4.86E+01	3.51E+01	1.34E+01		
473	1.49E+01	1.14E+01	6.22E+00		
Run 3		$x(SnBr_2) = 0.275$			
583	5.54E+03	6.51E+03	4.50E+03	1.74E+03	
563	4.04E+03	4.25E+03	2.61E+03	9.64E+02	
553	3.53E+03	2.56E+03	1.10E+03	2.88E+02	
543	2.02E+03	1.31E+03	4.38E+02	8.35E+01	
533	1.35E+03	6.64E+02	2.14E+02	3.73E+01	
523	6.56E+02	3.44E+02	1.14E+02	2.24E+01	
513	3.02E+02	1.42E+02	4.24E+01	6.46E+00	
503	6.65E+01	2.84E+01	7.91E+00		
493	1.36E+01				
Run 4		$x(SnBr_2) = 0.123$			
583	7.92E+02	3.15E+03	7.74E+03	7.55E+03	
573	6.77E+02	2.54E+03	6.16E+03	5.81E+03	
563	4.40E+02	1.79E+03	4.32E+03	4.08E+03	
553	1.35E+03	3.00E+03	3.90E+03	1.92E+03	
543	9.88E+02	1.93E+03	2.25E+03	1.04E+03	
533	6.60E+02	1.28E+03	1.47E+03	6.61E+02	
523	3.30E+02	6.38E+02	7.35E+02	3.38E+02	
513	2.39E+01	5.88E+01	7.80E+01	4.10E+01	
503	6.73E+01	1.54E+02	1.83E+02	1.01E+02	
493	2.73E+01	6.95E+01	7.68E+01	3.43E+01	
483	1.36E+01	2.65E+01	3.42E+01	1.49E+01	
Run 5		$x(SnBr_2) = 0.123$			
503	4.64E+02	3.40E+02	1.21E+02	3.08E+01	
584	1.72E+03	7.20E+03	1.16E+04	1.10E+04	
573	1.26E+03	5.03E+03	7.97E+03	7.65E+03	
563	3.04E+03	6.95E+03	6.38E+03	3.68E+03	
553	2.76E+03	5.31E+03	4.07E+03	2.01E+03	
543	2.05E+03	3.26E+03	2.24E+03	9.64E+02	
533	1.13E+03	1.66E+03	1.13E+03	4.77E+02	
523	7.33E+02	9.42E+02	5.48E+02	1.95E+02	
513	5.71E+02	5.75E+02	2.68E+02	8.30E+01	
503	3.02E+02	2.81E+02	1.15E+02	2.86E+01	
493	1.35E+02	1.19E+02	4.12E+01	9.94E+00	
483	5.54E+01	4.68E+01	1.64E+01		

3. Theoretical Approach and Computational Details

The geometries of the studied species were optimized by applying the second-order Møller−Plesset perturbation theory (MP2)[9] and density functional theory (DFT) methods.[10] No symmetry constraints were imposed during the optimization process, and geometry searches were carried out for a number of possible isomers to ensure the location of the global minimum. At the DFT level of theory the location of true minima was confirmed by frequency calculations. The density functional theory (DFT) approach has utilized the Becke's three-parameter functional[11] with the Vosko et al. local correlation part[12] and the Lee et al.[13] nonlocal part (abbreviated as B3LYP). All calculations were carried out using relativistic effective core potentials (RECPs) developed by the Stuttgart group.[14] Optimizations and frequency calculations were performed in the SDB-aug-cc-pVTZ basis set[15] from which the single f function characterized by the lowest exponent was removed. Additionally, the single point calculations were performed at the MP2 level in the extended SDB-aug-cc-pVQZ basis set[15] constituting the most advanced level of theory presented in this work. Because of the ionic nature of chemical bonds in the studied complexes, the application of selected basis sets was confirmed by the computation of the ionization potential of Sn and electron affinities of halogen atoms. The calculated ionization potential of tin (7.17 eV) agrees well with the experimental value (7.34 eV).[16] Theoretical values of electron affinities for Br (3.460 eV) and I (3.277 eV) also agree satisfactorily with the respective experimental data of 3.363 and 3.0590 eV.[16] The calculated values corrected for the spin−orbit effect are 3.155 eV for Br and 2.649 eV for I. Vibrational frequencies and thermodynamic properties of the studied complexes were calculated applying the ideal gas, rigid rotor, and harmonic oscillator approximations.[17]

The total interaction energy calculated at the MP2 level

$$\Delta E_{MP2} = E_{AB} - E_A - E_B \quad (1)$$

has been decomposed

$$\Delta E_{MP2} = \Delta E_{HF} + \epsilon_{MP}^{(2)} \quad (2)$$

into Hartree−Fock (HF) and correlation components ($\epsilon_{MP}^{(2)}$). The HF interaction energy decomposition was performed within the variational-perturbational scheme, corrected for the basis set superposition error (BSSE).[18] In the above scheme ΔE_{HF} is partitioned into electrostatic ($\epsilon_{el}^{(10)}$) and Heitler−London-exchange (ϵ_{ex}^{HL}) first-order components and the higher order delocalization (ΔE_{del}^{HF}) term. The delocalization energy accounts for the charge transfer, induction, and other higher order Hartree−Fock terms.[19] The correlation contribution $\epsilon_{MP}^{(2)}$ was also corrected for BSSE. The main contribution to it constitutes the second-order Hartree−Fock dispersion energy. The remaining terms giving significant contribution to $\epsilon_{MP}^{(2)}$ are correlation corrections to the HF components.[20]

The calculations were carried out using the Gaussian 98 suite of programs.[21] The interaction energy decomposition was performed applying the modified version[22] of the Gamess code.[23]

4. Results

4.1. Mass Spectrometric Studies. Table 1 summarizes ion intensities of dimeric species obtained in five runs by the Knudsen effusion mass spectrometry. The vapor composition over three studied samples differs significantly from each other due to the different chemical and phase compositions. The thermodynamic consistency of the calculated gaseous equilibria could be, therefore, checked due to their independence from the vapor composition.

The ionization of $Sn_2Br_xI_{4-x}$ complexes by electron bombardment leads to the formation of $Sn_2Br_yI_{3-y}^+$ fragment ions. The fragmentation of dimeric complexes to ions containing a single

Sn atom, such as $SnBr_2^+$ and SnI_2^+, cannot be ruled out, although these ions originate predominantly from monomeric species.[6] As shown in Table 1, each of the $Sn_2Br_yI_{3-y}^+$ ions can have only two neutral precursors. None of these ions is "pure", mainly originating from the single neutral species. This makes the assignment of these ions to their neutral precursors difficult and thereby also the thermochemical analysis of processes involving dimer species.

Studies of the fragmentation of $NaSnBr_nI_{3-n}$ complexes indicate[5] that the splitting off I atom is much more probable in comparison to the fragmentation by splitting off Br atoms. The same conclusion was drawn by Gietmann et al. in the case of the fragmentation of $HoBrI_2$, $HoBr_2I$ and $Ho_2Br_nI_{6-n}$ ($n = 1-5$) mixed gaseous species.[24] Alichanian and co-workers postulated the fragmentation of UCl_nBr_{4-n}(g) by splitting only the larger Br atom.[25] In the present study we performed, therefore, calculations of the gaseous equilibria involving the $Sn_2Br_xI_{4-x}$ species assuming that each of the $Sn_2Br_yI_{3-y}^+$ fragment ions originate only from the $Sn_2Br_yI_{4-y}$ neutral precursor, i.e., by splitting off the I atom. This assumption is denoted in Table 1 as full lines on the fragmentation scheme.

Let us consider the following gaseous anion-exchange reactions:

$$Sn_2Br_4 + Sn_2I_4 = 2Sn_2Br_2I_2 \quad (3)$$

$$Sn_2Br_3I + Sn_2BrI_3 = 2Sn_2Br_2I_2 \quad (4)$$

$$Sn_2Br_3I + Sn_2I_4 = Sn_2Br_2I_2 + Sn_2BrI_3 \quad (5)$$

$$Sn_2Br_2I_2 + Sn_2I_4 = 2Sn_2BrI_3 \quad (6)$$

The partial pressure $p(i)$ of species i at temperature T results from the relation[7]

$$p(i) = (kT\Sigma I(j,i))/\sigma(i) \quad (7)$$

where k is the pressure calibration factor, $I(j,i)$ is the intensity of j ions originating upon the electron bombardment of species i, and $\sigma(i)$ denotes the partial ionization cross section of molecule i giving j-ions. Adopting eq 7 for the gaseous anion-exchange reactions, eqs 3−6, one can write equilibrium constant $K_p°$ as an intensity quotient of ions originating from respective gaseous species. As an example for reaction 6 from the above considerations the equilibrium constant can be formulated as follows:

$$K_p°(6) = \frac{p(Sn_2BrI_3)^2}{p(Sn_2I_4)p(Sn_2Br_2I_2)} = C\frac{I(Sn_2BrI_2^+)^2}{I(Sn_2I_3^+)I(Sn_2Br_2I^+)} \quad (8)$$

The constant C contains the respective $\sigma(i)$ values of species involved in the reaction. As mentioned above, the $Sn_2Br_yI_{3-y}^+$ ion intensities in eq 8 are assumed to predominantly originate from $Sn_2Br_yI_{4-y}$(g). The respective intensity quotients can by formulated for reactions 3−5 as well. Once the real $K_p°(i)$ and C values remain constant for the different gas phase compositions, the respective ion intensity quotient is also expected to remain constant for different mass spectra in Table 1. We neglect here the temperature dependence of the equilibrium constants of reactions 3−6, which is justified for the anion-exchange processes.

The assumption of the origin of the $Sn_2Br_yI_{3-y}^+$ ion by analyzing mass spectra given in Table 1 has been checked in the following manner. The respective ion intensity quotients for reactions 3−6 were calculated for each experimental point by the use of total $Sn_2Br_yI_{3-y}^+$ ion intensities for the $Sn_2Br_yI_{4-y}$ species in each case. The total intensity of the $Sn_2Br_3^+$ ions was used for Sn_2Br_4(g) in reaction 3 and for Sn_2Br_3I(g) in reaction 4. Apart from the statistical scatter, we obtained almost constant values of $K_p°(4)$, $K_p°(5)$, and $K_p°(6)$, contrary to $K_p°(3)$. To get a better understanding of the meaning of this observation, we constructed graphs shown in Figure 1 a−d. All points in Table 1 are presented in the graphs as a dependence derived for reactions 3−6, from the ion intensity quotients representative for the respective $K_p°(i)$. The intensity quotient remains constant for mass spectra in Table 1 if the respective graph in Figure 1a−d shows linearity and crosses the zero point of the diagram. It follows from the experimental mass spectra that only $K_p°(3)$ does not fulfill these requirements. We conclude that the reason is the origin of $Sn_2Br_3^+$ ions predominantly from the Sn_2Br_3I molecule and not from Sn_2Br_4(g), as assumed for the computation of the ion intensity quotient representative for $K_p°(3)$.

If one neglects other fragmentation paths of $Sn_2Br_xI_{4-x}$ species in addition to these denoted in Table 1 as full lines, the values of $K_p°(4)-K_p°(6)$ and $\Delta_rG°(4)-\Delta_rG°(6)$ can be calculated from the experimental mass spectra. The ionization cross section term included in constant C is expected in each case to be nearly 1 if the additivity is applied for the $Sn_2Br_xI_{4-x}$ species. $K_p°$ values and Gibbs energies for reactions 4−6 at 550 K are presented in Tables 2 and 3, as an example. We have not considered here reaction 3, due to the necessity of dividing the total intensity of the $Sn_2Br_3^+$ ions between the Sn_2Br_4 and Sn_2Br_3I species, both leading to this fragment.

4.2. Quantum Chemical Calculations of $Sn_2Br_xI_{4-x}$(g) and $Sn_2Br_yI_{3-y}^+$. *4.2.1. Structure of Molecules and Ions.* The $SnBr_2$, SnI_2, and SnBrI monomers possess the nonlinear C_{2v} symmetry. The computed bond distances and angles closely reproduce the available experimental values[26] (Table 4). Geometries calculated at the most advanced (MP2/SBQ-aug-cc-pVQZ) level of theory applied in this work are only slightly different from those obtained in the SBQ-aug-cc-pVTZ basis set. This agreement gives us confidence in the optimized geometry of larger structures. The reasonable representation of bonding in monomers is confirmed by the calculated values of the vibrational frequencies being in the range expected from experiments for such studies.[26−29] A comparison between SnBrI and $SnBr_2$ and SnI_2 reveals the additivity of properties such as bond length, vibrational frequencies, and atomic charge distribution corresponding to Sn−Br and Sn−I bonds (Table 4).

The energetically lowest isomers of the Sn_2Br_4 and Sn_2I_4 complexes possess the chairlike conformation with two halogen and two tin atoms forming a four-membered ring with halogens located between metal atoms (bridged bonds) and two metal−halogen terminal bonds (Figure 2a). The ring is significantly deformed from the plane. Skeletons of compounds of the mixed $Sn_2Br_xI_{4-x}$ composition closely resemble structures of the homogeneous complexes. The terminal metal−halogen bonds are not equivalent. The a-terminal bond falls inside the ring (the "in" position), whereas the b-terminal bond is heading outside the ring (the "out" position, Figure 2a). For mixed substitutions the a-terminal atom is always bromine (Table 5). The terminal bond distances are longer by only a few hundred angstroms than the distances predicted for monomers. The bridged bonds are about 0.2 Å longer than the terminal bonds. The above conclusion agrees with the bond distance variation in many other substituted cyclic structures.[30] The search for isomers possessing a direct Sn−Sn bond was unsuccessful. The ethylene-like structure of Sn_2Br_4 is more than 300 kJ mol^{-1} above the ground state. This observation is in line with the

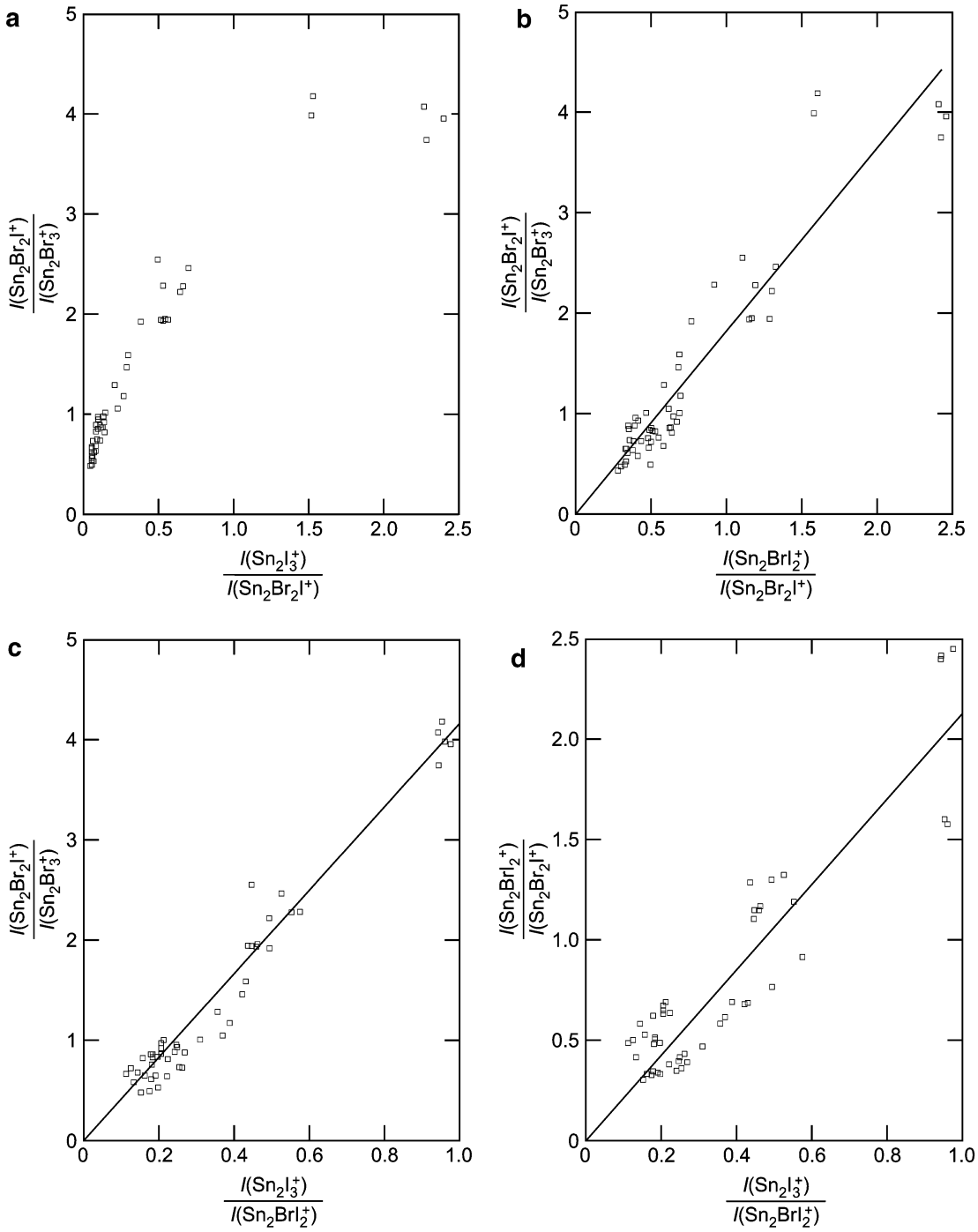

Figure 1. Experimental ion intensity ratios representative for (a) $K_p°(3)$, (b) $K_p°(4)$, (c) $K_p°(5)$, and (d) $K_p°(6)$ (see text).

TABLE 2: Equilibrium Constants, Thermochemical Functions, and Third Law Enthalpies for Gaseous Anion-Exchange Equilibria, Eqs 4−6, Obtained from Mass Spectrometric Data and Quantum Chemical Calculations

eq	$K_p°$-(550 K,exp)	$\Delta_rG°$(550 K,exp), J mol^{-1}	$\Delta_rS°$(298 K,theor), J mol^{-1} K^{-1}	$\Delta_rH°$(298 K), J mol^{-1} run 1	run 2	run 3	run 4	run 5	selected
4	1.81 ± 0.05	−2710	9.09	2199 ± 675	3250 ± 567	2637 ± 299	2419 ± 581	1051 ± 322	2311 ± 806
5	4.11 ± 0.07	−6460	2.94	−4436 ± 787	−5386 ± 510	−3276 ± 406	−4984 ± 349	−4242 ± 718	−4465 ± 803
6	2.18 ± 0.07	−3560	−6.16	−6641 ± 1161	−8810 ± 355	−5900 ± 288	−7409 ± 550	−5316 ± 511	−6815 ± 1365

available Raman spectra for Sn_2Cl_4 indicating the lack of bands characteristic for the metal−metal bond.[31]

The preferred dissociation of molecules takes place as the breaking of the b-terminal bond. Such a reaction leads to the complex with three halogen atoms involved in the bridged bonding between two tin atoms (Figure 2b). The $Sn_2Br_3^+$ and $Sn_2I_3^+$ cations form a trigonal bipyramid possessing perfect C_{3v} symmetry (Table 6). The value of the metal−halogen distance falls between the length of the terminal and bridged bonds of the neutral molecules.

4.2.2. Dimer Formation. The dimerization reaction proceeds with the concerted formation of two new metal−halogen bonds. The formation of the four-membered SnX_2Sn ring leads to four almost equivalent Sn−X bonds. Few perturbations in bridged

TABLE 3: Equilibrium Constants and Thermochemical Functions for Gaseous Anion-Exchange Equilibria Involving the $Sn_2Br_xI_{4-x}$ Dimeric Species at 550 K Obtained from Mass Spectrometric Data and Calculated by Quantum Chemical Methods

no.	reaction	$K_p°$(550 K,exp)	$\Delta_rG°$(550 K,exp), J mol^{-1}	$\Delta_rS°$(298 K,theor), J mol^{-1} K^{-1}	$\Delta_rH°$,[a] J mol^{-1}
1	$Sn_2(Br_2)Br_2 + Sn(I_2)I_2 = 2\ Sn_2(Br_2)I_2$			10.46	
2	$Sn_2(Br_2)BrI + Sn_2(BrI)I_2 = 2\ Sn_2(Br_2)I_2$	1.81 ± 0.05	−2710	9.09	2290
3	$Sn_2(Br_2)BrI + Sn(I_2)I_2 = Sn_2(Br_2)I_2 + Sn_2(BrI)I_2$	4.11 ± 0.07	−6460	2.94	−4850
4	$Sn_2(Br_2)I_2 + Sn(I_2)I_2 = 2\ Sn_2(BrI)I_2$	2.18 ± 0.07	−3560	− 6.16	−6950
5	$Sn_2(Br_2)Br_2 + Sn(I_2)I_2 = Sn_2(Br_2)BrI + Sn_2(BrI)I_2$			1.37	

[a] Valid for the temperature range 298−550 K.

TABLE 4: Bond Distances (r in Angstroms), Angles (α in Degrees), Vibrational Frequencies (ν in cm^{-1}), and Atomic Charge (q in electrons) at the B3LYP/SDB-aug-cc-pVTZ Level and MP2 Calculations in SDB-aug-cc-pVTZ and SDB-aug-cc-pVQZ Basis Sets

		bond distances			vibrational frequencies			atomic charges	
molecule	method	r(Sn−Br)	r(Sn−I)	α	ν_1	ν_2	ν_3	q(Br)	q(I)
$SnBr_2$	B3LYP	2.552		100.0	233.4	76.7	224.6	−0.277	
	MP2[a]	2.523		98.6				−0.291	
	MP2[b]	2.517		98.1					
	Expt.	2.504[c]		98.6[c]	261,[c] 244[d]	81,[c] 80[e]	243,[c] 231[d]		
SnBrI	B3LYP	2.554	2.764	100.6	182.9	66.9	227.2	−0.278	−0.142
	MP2[a]	2.526	2.732	99.0				−0.287	−0.143
	MP2[b]	2.520	2.728	98.4					
SnI_2	B3LYP		2.767	101.3	183.7	57.3	179.6		−0.143
	MP2[a]		2.735	99.4					−0.142
	MP2[b]		2.730	98.8					
	exp		2.699[c]	103.5[c]	212,[c] 232[f]	61,[c] 61[f]	227,[c] 240[f]		

[a] In SDB-aug-cc-pVTZ. [b] In SDB-aug-cc-pVQZ. [c] Reference 26. [d] Reference 27. [e] Reference 28. [f] Reference 29.

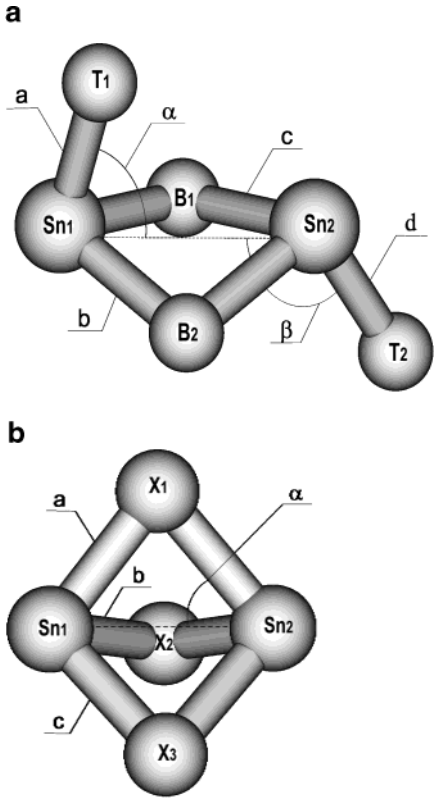

Figure 2. Schematic representation of (a) $Sn_2Br_xI_{1-x}$(g) and (b) $Sn_2Br_yI_{3-y}^+$. (For parameters, see Tables 4 and 5).

bonding are due to nonequivalency of the terminal bonds. The lowest electronic excited states are located more than 3 eV (B3LYP level) above the ground state. Consequently, we expect that the spin−orbit corrections are not significant. The other relativistic contributions are accounted for by applying relativistic effective core potentials. The dimerization energy is the highest in the iodine substituted molecule Sn_2I_4. The dimerization of $SnBr_2$ is about 10 kJ mol^{-1} smaller (Table 7).

The total dimerization energy is dominated by the correlation energy contribution. The Hartree−Fock energy accounts for less than one-third of the total energy. More importantly, the correlation energy reverses the order of stability of the molecules. The DFT/B3LYP approach only partially accounts for correlation effects, and compared to the MP2 results, the difference is qualitative. The overall energy of the dimerization reaction is well represented by additive contributions of single bonds. The calculated entropy of the reaction indicates the higher rigidity of the dimers. Due to the size of the iodine atoms, molecules with a larger number of iodine atoms are characterized by a larger negative contribution to the total entropy of dimerization. The experimental values of enthalpy and entropy of formation are reasonably reproduced by calculations (Table 7). However, the predicted value of the dissociation enthalpy of Sn_2I_4 is higher than the corresponding enthalpy of Sn_2Br_4, which is in disagreement with experimental data. The calculated difference is not large and falls within the expected range of error for theoretical predictions. The larger ΔS predicted for Sn_2I_4, indicates that differences between the stability (ΔG) of studied molecules will narrow and may be reversed at higher temperatures.

A comparison between the total interaction energy values and the dimer dissociation energy indicates the important contribution of the geometry relaxation term to the dissociation energy of dimers. The relaxation of monomers reverses the order of stabilization energies of the dimer. The interaction energy partitioning indicates the significant differences between the Sn−Br and Sn−I bonds. The Sn−Br bridged bond is stabilized mostly by electrostatic forces, whereas the dispersion contribution is the most important component of Sn−I interactions (Table 8). In both cases the HF interactions are almost equal to the electrostatic forces with the exchange repulsion canceling almost entirely the energy delocalization term. In the first-order approximation the interaction energy components may be

TABLE 5: Structural Parameters (Definition in Figure 2a) of $Sn_2Br_xI_{4-x}$ Complexes ($x = 0-4$) Optimized at the MP2/SBQ-aug-cc-pVTZ Level[a]

n	molecule	a-terminal bond		b-bridge bond		α-angle		c-bridge bond		d-terminal bond		*β*-angle		dihedral	
1	$Sn_2(Br_2)Br_2$	Br−Sn	2.562	Sn−Br	2.807	Br−Sn−Sn	68.7	Br−Sn	2.807	Sn−Br	2.536	Sn−Sn−Br	117.4	Sn−Br−Br−Sn	133.5
2	$Sn_2(Br_2)BrI$	Br−Sn	2.561	Sn−Br	2.808	Br−Sn−Sn	68.7	Br−Sn	2.808	Sn−I	2.749	Sn−Sn−I	118.1	Sn−Br−Br−Sn	133.5
3	$Sn_2(BrI)Br_2$	Br−Sn	2.566	Sn−I	2.961	Br−Sn−Sn	67.2	Br−Sn	2.806	Sn−Br	2.541	Sn−Sn−Br	119.7	Sn−Br−I−Sn	129.8
4	$Sn_2(Br_2)I_2$	I−Sn	2.776	Sn−Br	2.806	I−Sn−Sn	70.4	Br−Sn	2.806	Sn−I	2.750	Sn−Sn−I	117.7	Sn−Br−Br−Sn	134.4
5	$Sn_2(I_2)Br_2$	Br−Sn	2.570	Sn−I	3.010	Br−Sn−Sn	65.8	I−Sn	3.010	Sn−Br	2.546	Sn−Sn−Br	122.2	Sn−I−I−Sn	126.1
6	$Sn_2(BrI)BrI$	Br−Sn	2.564	Sn−I	2.964	Br−Sn−Sn	67.3	Br−Sn	2.807	Sn−I	2.753	Sn−Sn−I	120.4	Sn−Br−I−Sn	129.9
7	$Sn_2(BrI)I_2$	I−Sn	2.779	Sn−Br	2.756	I−Sn−Sn	69.0	I−Sn	3.010	Sn−I	2.755	Sn−Sn−I	120.1	Sn−I−Br−Sn	130.8
8	$Sn_2(I_2)BrI$	Br−Sn	2.568	Sn−I	3.009	Br−Sn−Sn	65.9	I−Sn	3.009	Sn−I	2.759	Sn−Sn−I	122.9	Sn−I−I−Sn	126.2
9	$Sn_2(I_2)I_2$	I−Sn	2.782	Sn−I	3.006	I−Sn−Sn	67.7	I−Sn	3.006	Sn−I	2.760	Sn−Sn−I	122.6	Sn−I−I−Sn	127.1

[a] Distances in angstroms, angles in degrees. Information regarding vibrational frequencies is given as Supporting Information.

TABLE 6: Structural Parameters (Definition in Figure 2b) for $Sn_2Br_yI_{3-y}^+$ Complexes ($y = 0-3$) Optimized at the MP2/SBQ-aug-cc-pVTZ Level[a]

n	cation	a-bridge bond		b-bridge bond		c-bridge bond		α-angle		*β*-angle		*γ*-angle	
1	$Sn_2Br_3^+$	Sn−Br	2.746	Sn−Br	2.746	Sn−Br	2.746	Br−Sn−Sn	50.1	Br−Sn−Sn	50.1	Br−Sn−Sn	50.1
2	$Sn_2Br_2I^+$	Sn−I	2.987	Sn−Br	2.785	Sn−Br	2.785	I−Sn−Sn	53.2	Br−Sn−Sn	50.0	Br−Sn−Sn	50.0
3	$Sn_2BrI_2^+$	Sn−Br	2.750	Sn−I	2.947	Sn−I	2.947	Br−Sn−Sn	49.4	I−Sn−Sn	52.6	I−Sn−Sn	52.6
4	$Sn_2I_3^+$	Sn−I	2.947	Sn−I	2.947	Sn−I	2.947	I−Sn−Sn	52.3	I−Sn−Sn	52.3	I−Sn−Sn	52.3

[a] Distances in angstroms, angles in degrees.

TABLE 7: Energies (kJ mol^{-1}), Enthalpies (kJ mol^{-1}), and Entropies (J mol^{-1} K^{-1}) of the Dimerization Reactions Calculated at Different Levels of Theory and Comparison with Experiment[a]

n	dimerization reaction	ΔE_o(B3LYP)	ΔH(B3LYP)	ΔS(B3LYP) (exp)	ΔE_o(MP2)[b]	ΔE_o(HF)[c]	ΔE_o(MP2)[c]	ΔH(MP2)[c,d] (exp)
1	$2SnBr_2 = Sn_2(Br_2)Br_2$	−69.6	−64.7	−141.3	−109.1	−44.0	−115.3	−110.4
				(-153.8 ± 8.8)[6]				(-106.8 ± 3.6)[6]
2	$SnBr_2 + SnBrI = Sn_2(Br_2)BrI$	−68.6	−63.7	−147.4	−109.9	−42.8	−116.2	
3	$SnBr_2 + SnBrI = Sn_2(BrI)Br_2$	−68.6	−63.7	−147.5	−111.1	−40.9	−118.3	
4	$2SnBrI = Sn_2(Br_2)I_2$	−67.3	−62.4	−153.6	−111.4	−40.8	−118.0	
5	$2SnBrI = Sn_2(I_2)Br_2$	−68.2	−63.3	−153.4	−114.4	−38.6	−122.5	
6	$SnBr_2 + SnI_2 = Sn_2(BrI)BrI$	−67.4	−62.5	−147.1	−111.4	−40.3	−119.9	
7	$2SnBrI = Sn_2(BrI)BrI$	−67.9	−63.0	−152.9	−112.6	−39.5	−118.7	
8	$SnBrI + SnI_2 = Sn_2(BrI)I_2$	−66.4	−61.5	−153.1	−115.4	−37.8	−121.5	
9	$SnBrI + SnI_2 = Sn_2(I_2)BrI$	−67.3	−62.3	−152.8	−115.4	−37.5	−123.7	
10	$2SnI_2 = Sn_2(I_2)I_2$	−66.2	−61.2	−153.4	−117.7	−34.4	−126.4	−121.4
				(-158.3 ± 10.2)[32]				(-101.0 ± 4.4)[32]

[a] Data are given for standard pressure of 1 bar and 298.15 K [b] In the SBQ-aug-cc-pVTZ basis set. [c] In the SBQ-aug-cc-pVQZ basis set. [d] The enthalpy correction to energy was adopted from B3LYP calculations.

TABLE 8: Interaction Energy Components, in kJ mol^{-1}, for the Dimerization of Tin Dihalides

n	molecule	$\epsilon_{el}^{(10)}$	ΔE_{ex}^{HL}	ΔE_{del}^{HF}	ΔE_{HF}	$\epsilon_{MP}^{(2)}$	ΔE_{MP2}
1	$Sn_2(Br_2)Br_2$	−108.47	379.14	−364.59	−93.94	−57.24	−151.81
2	$Sn_2(Br_2)BrI$	−108.96	382.17	−365.05	−91.84	−58.86	−150.69
3	$Sn_2(BrI)Br_2$	−89.33	381.83	−376.31	−91.84	−64.38	−148.19
4	$Sn_2(Br_2)I_2$	−108.41	388.71	−368.49	−88.19	−62.35	−150.54
5	$Sn_2(I_2)Br_2$	−73.33	384.01	−386.42	−75.74	−71.88	−147.62
6	$Sn_2(BrI)BrI$ ($SnBrI/SnBrI$)[a]	−93.23	385.25	−376.06	−84.05	−65.98	−150.03
7	$Sn_2(BrI)BrI$ ($SnBr_2/SnI_2$)[a]	−89.71	383.67	−375.13	−81.61	−64.38	−148.19
8	$Sn_2(BrI)I_2$	−92.54	391.72	−379.15	−79.97	−69.66	−149.62
9	$Sn_2(I_2)BrI$	−73.71	387.60	−387.53	−73.64	−73.70	−147.34
10	$Sn_2(I_2)I_2$	−72.94	395.65	−392.62	−69.91	−77.97	−147.88

[a] Assumed monomers.

considered as additive, and the interaction energy depends on the number of Br and I atoms in the formed ring. The electron charge distribution confirms the interaction energy components picture (Table 9). The atomic charge on the iodine atom (in the bridged bond) is close to zero indicating that the binding is dominated by dispersion and induction (represented by the delocalization term) interaction energy decomposition terms.

The total energy of isomers containing bromine and iodine indicates the higher stabilization of molecules with bridged Sn−I and terminal Sn−Br bonds. The energy differences in pairs of isomers ($Sn_2(BrI)Br_2$, $Sn_2(Br_2)BrI$), ($Sn_2(I_2)Br_2$, $Sn_2(Br_2)I_2$), and ($Sn_2(I_2)BrI$, $Sn_2(BrI)I_2$) are 2.1, 4.51, and 2.2 kJ mol^{-1}, respectively. The effect of switching on one (I, Br) pair is about 2 kJ mol^{-1}. Although systematic, the energy difference is negligible, and at higher temperatures isomers will constitute the equilibrium mixture. Theoretical data obtained for dimeric species resulted also in the computation of entropy changes for anion-exchange processes, eqs 4−6. The values of $\Delta_r S°$(298 K,theor) are included in Tables 2 and 3. Third law enthalpies, $\Delta_r H°$(298 K), of reactions were evaluated in each run from experimental $\Delta_r G°(T)$ and theoretical $\Delta_r S°$(298 K) values. Results of the third law evaluation are given in Tables 2 and 3.

TABLE 9: Atomic Charges for $Sn_2Br_xI_{4-x}$ ($x = 0-4$) Calculated within the Mulliken Population Analysis Representing the MP2 Electronic Density[a]

		Sn1	bridged halogens				terminal halogens				Sn2
n	molecule	charge	B_1	charge	B_2	charge	T_1	charge	T_2	charge	charge
1	$Sn_2(Br_2)Br_2$	0.449	Br	−0.188	Br	−0.188	Br	−0.282	Br	−0.313	0.522
2	$Sn_2(Br_2)BrI$	0.441	Br	−0.181	Br	−0.181	Br	−0.289	I	−0.179	0.390
3	$Sn_2(BrI)Br_2$	0.350	I	−0.031	Br	−0.177	Br	−0.276	Br	−0.312	0.447
4	$Sn_2(Br_2)I_2$	0.307	Br	−0.176	Br	−0.176	I	−0.160	I	−0.180	0.385
5	$Sn_2(I_2)Br_2$	0.255	I	−0.023	I	−0.023	Br	−0.272	Br	−0.313	0.379
6	$Sn_2(BrI)BrI$	0.344	I	−0.027	Br	−0.171	Br	−0.284	I	−0.182	0.320
7	$Sn_2(BrI)I_2$	0.215	I	−0.024	Br	−0.167	I	−0.157	I	−0.184	0.316
8	$Sn_2(I_2)BrI$	0.250	I	−0.020	I	−0.020	Br	−0.279	I	−0.186	0.255
9	$Sn_2(I_2)I_2$	0.126	I	−0.017	I	−0.017	I	−0.156	I	−0.190	0.252

[a] Charges in electrons.

TABLE 10: Energies (kJ mol^{-1}), Enthalpies (kJ mol^{-1}), and Entropies (J mol^{-1} K^{-1}) of the Dissociation of the Terminal Bond (Reaction 9) Calculated at Various Levels of Theory and Applying the Experimental Electron Affinity of Halogens[a]

n	dissociation reaction	ΔE_o(B3LYP)	ΔH(B3LYP)	ΔS(B3LYP)	ΔE_o(MP2)[b]	ΔE_o(HF)[c]	ΔE_o(MP2)[c]
1	$Sn_2(Br_2)Br_2 = Sn_2(Br_3)^+ + Br$	898.4	892.2	78.3	908.8	886.6	909.7
2	$Sn_2(Br_2)BrI = Sn_2(Br_2I)^+ + Br$	885.0	883.7	83.4	901.8	882.8	902.9
3	$Sn_2(Br_2)BrI = Sn_2(Br_3)^+ + I$	830.0	824.4	76.4	847.7	814.9	850.6
4	$Sn_2(BrI)Br_2 = Sn_2(Br_2I)^+ + Br$	885.0	883.6	83.5	903.0	881.0	905.0
5	$Sn_2(Br_2)I_2 = Sn_2(Br_2I)^+ + I$	821.8	820.5	81.7	841.3	810.2	841.9
6	$Sn_2(I_2)Br_2 = Sn_2(BrI_2)^+ + Br$	879.4	888.0	83.9	852.2	875.5	899.6
7	$Sn_2(BrI)BrI = Sn_2(BrI_2)^+ + Br$	879.1	877.7	83.5	895.4	877.2	897.0
8	$Sn_2(BrI)BrI = Sn_2(Br_2I)^+ + I$	822.5	821.2	81.0	842.5	809.7	843.8
9	$Sn_2(BrI)I_2 = Sn_2(BrI_2)^+ + I$	816.3	815/0	81.6	835.9	804.9	837.1
10	$Sn_2(I_2)BrI = Sn_2(I_3)^+ + Br$	873.4	871.9	83.4	889.2	871.6	891.3
11	$Sn_2(I_2)BrI = Sn_2(BrI_2)^+ + I$	817.1	815.8	81.3	837.4	804.6	839.3
12	$Sn_2(I_2)I_2 = Sn_2(I_3)^+ + I$	810.9	809.6	81.9	830.7	799.7	832.4

[a] Thermodynamic functions are given for the standard pressure of 1 bar and 298.15 K. [b] In the SBQ-aug-cc-pVTZ basis set. [c] In the SBQ-aug-cc-pVQZ basis set.

Arithmetical mean enthalpies obtained in respective runs are also reported. All uncertainties given in Tables 2 and 3 are standard deviations of mean.

4.2.3. Properties of Terminal Bonds. The studied structures of $Sn_2Br_xI_{4-x}$ molecules possess two nonequivalent positions "in" and "out" for halogens bonded by terminal bonds (Figure 2a). The different environment of both terminal atoms significantly influences their properties. An atom in the "in" position has closer contacts with the ring atoms than atoms of the "out" halogen. Its negative charge is much smaller compared to the "out" halogen as well as compared to the atomic charge distribution in the monomer (Table 9). The "out" bonds are more ionic and closely resemble the bonding in monomers.

The dissociative fragmentation of dimeric species upon electron bombardment proceeds through the reaction

$$Sn_2Br_xI_{4-x} + e = Sn_2Br_yI_{3-y}^+ + Br\ (or\ I) + 2e \qquad (9)$$

The dissociation of the halogen from the dimer molecule takes place from the terminal "out" bond. The positive hole left after the dissociation is closed due to the formation of the third bridged bond by the terminal "in" halogen. The dissociation process leads to cations directly observed in the mass spectrum. Information concerning the energetics of this reaction supports the interpretation of the mass spectra. The energies of dissociation reactions exhibit a number of regularities. The highest dissociation energy is found in Sn_2Br_4 and the lowest in Sn_2I_4. The Sn−Br terminal bonds are more stable (the range of 909−890 kJ mol^{-1}) than Sn−I bonds (the range of 832−850 kJ mol^{-1}) (Table 10). The bridged bonds influence the strength of the terminal bonds. Iodine atoms forming bridged bonds lead to a lower dissociation energy of the terminal bonds. The influence is additive considering the number of bridged iodines (or bromines). For Br dissociating from the sequence of molecules $Sn_2(Br_2)Br_2$, $Sn_2(Br_2)BrI$, $Sn_2(BrI)BrI$, and $Sn_2(I_2)BrI$, where zero, one, two, and three bridged iodine bonds are formed in the cation, the dissociation energies are 905.6, 903.0, 897.0, and 891.3 kJ mol^{-1}, respectively. The presence of iodine in the bridge lowers the energy of the terminal bond dissociation by approximately 6 kJ mol^{-1}. Analogically, for the molecular series $Sn_2(Br_2)BrI$, $Sn_2(BrI)BrI$, $Sn_2(I_2)BrI$, and $Sn_2(I_2)I_2$, the dissociation energy of the Sn−I terminal bond systematically decreases (850.6, 843.8, 839.3, 832.4 kJ mol^{-1}) with the increasing number of Sn−I bridged bonds. The terminal bonds are well described at the HF level. The correlation contribution does not change the dissociation energy significantly. The atomic charges indicate the ionic nature of the terminal bonds.

5. Discussion and Conclusions

Two "pure" and three "mixed" dimeric species are present in the equilibrium vapor of the $SnBr_2-SnI_2$ system in addition to $SnBr_2$, SnBrI, and SnI_2 monomers being the major species.[6] The $Sn_2Br_xI_{4-x}$ molecules possess a chairlike structure with a four-membered SnX_2Sn nonplanar ring (bridged bonds) and two nonequivalent terminal Sn−X bonds (Figure 2a). The halogen atoms forming terminal bonds assume "in" and "out" positions relative to the ring. For different halogens occupying the terminal positions, the most stable geometry is adapted by isomers with Br in the "in" position and with I heading outside the skeleton.

The dimers are formed due to the concerted formation of additive metal−halogen bonds leading to the four-membered SnX_2Sn ring. The dimerization energy is dominated by the correlation energy contribution. Such forces are more important in iodine compounds, and the Sn_2I_4 dimer is more stable than Sn_2Br_4. The energy of dimerization is significantly influenced by the monomer relaxation due to the reaction. The interaction energy decomposition as well as the atomic charge distribution

indicates the significant differences between the Sn−Br and Sn−I bonds. The character of the Sn−Br bond is ionic, whereas Sn−I possesses a more covalent nature. For halogen-mixed species, the Sn_2Br_3I, $Sn_2Br_2I_2$, and Sn_2BrI_3, isomers with I involved in bridge bonding and Br in a terminal position are more stable in comparison to other structures. Anion-exchange reactions, eqs 4−6, are characterized by low enthalpies of 2−7 kJ mol^{-1} (Tables 2 and 3). This observation is understable due to the same total number of Sn−Br and Sn−I bonds existing in dimeric reagents on the left and right sides of each process. The high temperature equilibria between gaseous dimeric species result, therefore, mainly from respective entropy changes.

The dimeric species were identified by detecting the $Sn_2Br_yI_{3-y}^+$ fragment ions that originated by the dissociative fragmentation of neutral precursors with splitting off the single halogen atom. Such a fragmentation path is typical for gaseous metal halide species. In many cases fragments possessing one halogen atom less than the parent molecule are the most abundant in the mass spectrum of the metal halide complex (see, e.g., refs 4, 5, and 33). For minor species no signal for molecular ions is usually recorded, probably due to its low stability. The halogen atom dissociates preferably from the "out" terminal bond. The created halogen hole is healed by the formation of the third bridged bond (Figure 2b). The energetics of the dissociation is influenced by the composition of the bridged bonds. The iodine atoms constituting bridged bonds lower the energy of the reaction. The bonding in the studied moieties is characterized by the significant additivity of the properties.

The preferable splitting off of a larger halogen, i.e., an iodine atom observed as the fragmentation of mixed $Sn_2Br_xI_{4-x}$ species due to electron bombardment, agrees with the previous studies of the fragmentation of mixed halogen complexes.[5,24,25] It is quite understandable for the Sn_2BrI_3 molecule where the iodine atom occupies the "out" terminal position in the most stable I-bridged isomer (Table 10). As indicated by quantum chemical calculations, the slightly larger stability of I-bridged $Sn_2Br_xI_{4-x}$ isomers suggests that Sn_2Br_3I and $Sn_2Br_2I_2$ dimers are predominantly represented by species without I atoms in the "out" terminal positions ($Sn_2(BrI)Br_2$ and $Sn_2(I_2)Br_2$). The most probable explanation for this contradiction is the shift of isomer equilibria toward the Br-bridged species with iodine in the "out" terminal position at higher temperatures. This can be a result of the entropy effect considering the low energy difference between Br- and I-bridged isomers. Equilibration between the different $Sn_2Br_xI_{4-x}$(g) isomers can be easily achieved through dynamic dissociation−association processes, for instance:

$$Sn_2(Br_2)I_2(g) \leftrightarrows 2SnBrI(g) \leftrightarrows Sn_2(BrI)BrI(g)$$

Acknowledgment. This work was facilitated in part by the Polish State Committee for Scientific Research under Grant 3 T09A 020 19, NSF Grant No. 9805465 & 9706268, ONR Grant No. N00014-98-1-0592, and the Army High Performance Computing Research Centre under the auspices of the Department of the Army, Army Research Laboratory cooperative agreement number DAAH04-95-2-0003/contract number DAAH04-95-C-0008. This work does not necessarily reflect the policy of the government, and no official endorsement should be inferred. We thank the Mississippi Centre for Supercomputing Research, Poznan and Wroclaw Supercomputing and Networking Centres, and the Interdisciplinary Centre for Mathematical and Computational Modeling of Warsaw University for a generous allotment of computer time.

Supporting Information Available: Data supporting Table 5, include vibrational frequencies and moments of inertia of studied dimers. This information is available free of charge via Internet at http://pubs.acs.org.

References and Notes

(1) Hilpert, K.; Niemann, U. *Thermochim. Acta* **1997**, *299*, 49.
(2) Hilpert, K. *J. Electrochem. Soc*. **1989**, *136*, 2099.
(3) Groen, C. P.; Oskam, A.; Kovacs, A. *Inorg. Chem*. **2003**, *42*, 851.
(4) Miller, M. *Int. J. Mass Spectrom. Ion Processes* **1984**, *61*, 293.
(5) Miller, M.; Niemann, U.; Hilpert, K. *J. Electrochem. Soc*. **1994**, *141*, 2774.
(6) Hilpert, K.; Miller, M.; Ramondo, F. *J. Phys. Chem*. **1991**, *95*, 7261.
(7) Hilpert, K. *Rapid Commun. Mass Spectrom*. **1991**, *5*, 175.
(8) Thevet, F.; Dagron, C.; Flahaut, J. *C. R. Acad. Sci., Ser. C* **1974**, *278*, 1223.
(9) Møller C.; Plesset, M. S. *Phys. Rev*. **1934**, *46*, 618.
(10) Parr R. G.; Yang, W. *Density-Functional Theory of Atoms and Molecules*; Oxford University Press: New York, 1994.
(11) Becke, D. *J. Chem. Phys*. **1993**, *98*, 5648.
(12) Vosko, S. H.; Wilk, L.; Nusiar, M. *Can. J. Phys*. **1980**, *58*, 1200.
(13) Lee, C.; Yang, W.; Parr, R. G. *Phys. Rev. B* **1988**, *37*, 785.
(14) Bergner, A.; Dolg, M.; Kuechle, W.; Stoll, H.; Preuss, H. *Mol. Phys*. **1993**, *80*, 1431.
(15) Martin, J. M. L.; Sundermann, A. *J. Chem. Phys*. **2001**, *114*, 3408.
(16) *CRC Handbook of Chemistry and Physics*, 83rd ed.; Lide, D. R., Ed.; CRC Press: Boca Raton, FL, 2002.
(17) Davidson, N. *Statistical Mechanics*; McGraw-Hill: New York, 1962.
(18) Sokalski, W. A.; Roszak, S.; Pecul, K. *Chem. Phys. Lett*. **1988**, *153*, 153.
(19) Jeziorski, B.; van Hemert, M. C. *Mol. Phys*. **1976**, *31*, 713.
(20) Chalasinski, G.; Szczesniak, M. M. *Mol. Phys*. **1988**, *63*, 205.
(21) Frisch, M. J.; Trucks, G. W.; Schlegel, H. B.; et al. *Gaussian 98*, revision A.4; Pittsburgh, PA, 1998.
(22) Gora, R. W.; Bartkowiak, W.; Roszak, S.; Leszczynski, J. *J. Chem. Phys*. **2002**, *117*, 1031.
(23) Schmidt, M. S.; Baldridge, K. K.; Boatz J. A.; et al. *J. Comput. Chem*. **1993**, *14*, 1347.
(24) Gietmann, C.; Hilpert, K.; Nickel, H. *Ber. Forschungszentr. Juelich No*. **1997**, 3337.
(25) Alichanian, A. S.; Malkierova, I. P.; Sevastianov, V. G.; Juldaszev, F.; Gorgoraki V. I. *Vysokoch. Veshchestva* **1988**, *1*, 85.
(26) Nasarenko, A. Y.; Spiridonov, V. P.; Butayev, B. S.; Zasorin, E. Z. *J. Mol. Struct*. **1985**, *119*, 263.
(27) Ozin G. A.; Voet, A. V. *J. Chem. Phys*. **1972**, *56*, 4768.
(28) Beattie I. R.; Perry, R. O. *J. Chem. Soc. A* **1970**, 2429.
(29) Brewer, L.; Somayalulu, G. R.; Brackett, E. *Chem. Rev*. **1963**, *68*, 111.
(30) *Stereochemical Applications of Gas-Phase Electron Diffraction, Part B*; Hargittai, I., Hargittai, M., Eds.; VCH Publishers: New York, 1988; p 383.
(31) Fields, M.; Devonshire, R.; Edwards, H. G. M.; Fawcett, V. *Spectrochim. Acta A* **1995**, *51*, 2249.
(32) Hilpert, K.; Bencivenni, L.; Saha, B. *Ber. Bunsen-Ges. Phys. Chem*. **1985**, *89*, 1292.
(33) Hastie, J. W. *Chemical Vapor Transport and Deposition*, in *High-Temperature Vapors, Ser. Science and Technology*; Academic Press: New York, 1975; 91−211.